

## Application of new organoclays for the adsorption of bemacide dyes from aqueous solutions

Benamar Makhoukhi

Laboratory of Separation and Purification Technologies, Tlemcen University, BP 119, Algeria, Tel. +213 775008003, email: benamarmakh@yahoo.fr (B. Makhoukhi)

Received 24 December 2015; Accepted 5 February 2018

### ABSTRACT

Clay ion-exchange using bismidazolium salts (BuBIM) could provide organophilic clays materials that allow effective retention of polluting dyes. The present investigations deal with bentonite (Bt) modification using (ortho, meta and para) bisimidazolium cations and attempts to remove a synthetic textile dyes, such as (bemacide-Yellow, bemacide-Red and bemacide-Blue) by adsorption, from aqueous solutions. Adsorption tests applied to Bemacide dyes revealed a significant increase of the maximum adsorption capacity from ca. 13–27 to 125–168 mg·g<sup>-1</sup> after intercalation. The highest adsorption level was noticed for bemacide-Yellow dye on the p.BuBIM–Bt. The kinetics data were analyzed using pseudo-first order and pseudo-second order models. It was best described by the pseudo-first order model. The isotherm data were investigated according to Langmuir and Freundlich equations.

*Keywords:* Bentonite; Organoclay; Dyes; Isotherm models; Adsorption; Kinetic parameters

### 1. Introduction

Synthetic dyes can be found in the wastewater from various industries like paper, leather, printing, laundry, tannery, rubber, plastic, painting and textiles [1]. Wastewater discharges into rivers and natural streams from the industries that use dyes poses stark environmental problems. Even minor quantities of dyes can colour huge water bodies, which influences aesthetic merit and decreases light penetration needed for photosynthesis. Furthermore, many of dyes are toxic or carcinogenic [2]. Untreated disposal of this colored water into receiving water body causes severe damages to the human bodies and also to aquatic life [3]. Thus, the removal of colour dyes from waste water before they are contacted with unpolluted natural water bodies are currently one of the major problems faced by the textile dyeing industry.

Many approaches have been developed for decontamination of water, e.g. precipitation, electro dialysis, adsorption, filtration, coagulation, oxidation and membrane

separation. However, adsorption is known to be one of the most effective techniques to eliminate dyes from water. Adsorption phenomenon in solution systems plays a vital role in many areas of practical environmental technology, which are mainly in water and waste water treatment due to several advantages such as high efficiency, simple operation and easy recovery/reuse of adsorbent [4].

Activated carbon has been familiarized as adsorbent due to its great sorption capacity for the dyes [5]. However the high cost has led us seeking for low-cost sorbents. Recently, low-cost materials such as fly ash, natural zeolite, red mud and coir pith accepted vital interest for wastewater treatment [6–9]. In this regard, montmorillonite-rich materials like bentonites exhibit highly interesting properties, e.g. high specific surface area, cation-exchange capacity (CEC), porosity, and tendency to retain water or other polar and non-polar compounds. Some of these properties can easily be improved through acid activation [10].

Acid dyes are the most problematic due to their bright colour, acidic and water soluble reactive characteristics. Several studies have been executed on adsorption of basic dyes by clay minerals [11]. However, there is very little works

\*Corresponding author.

on adsorption of acidic dyes [12]. Generally, the adsorption capacity for anionic dyes is much lower than for cationic dyes, as result of weak attractions between acidic charges on the dyes and the negative surface of clay.

Bentonite comprises of one octahedral alumina sheet lying between two tetrahedral layers of silica. The permanent negative charge of bentonite is attributed to the isomorphous replacement of  $\text{Al}^{3+}$  for  $\text{Si}^{4+}$  in the tetrahedral layer and  $\text{Mg}^{2+}$  for  $\text{Al}^{3+}$  in the octahedral layer. This negative charge is balanced by the presence of replaceable cations ( $\text{Ca}^{2+}$ ,  $\text{Na}^+$ , etc.) in the lattice structure, which enhance adsorbing cationic pollutants [13]. Although, bentonite weakly adsorbs acidic contaminants due to repulsion force between the anion and the negative charge on the surface of the bentonite [14]. Several authors have informed the use of bentonite modified and organo bentonite, the surface of the natural clays has to be modified by a cationic surfactant for the dye adsorption experiments. By the ion-exchange mechanism, the inorganic cation could be exchanged by the organic surfactant cation. The modification of clay surface is called as organoclay to cause to transform organophobic to strongly organophilic and therefore the adsorption capacity increases to compare with natural clay mineral and it can be used as an adsorbent for the adsorption of dyes. This kind of surfactant modified organobentonite has been used extensively for a wide variety of environmental applications [15].

The aim of the present work is to investigate the possibility of new organo-bentonites as an adsorbent for removal of bemacide dyes, which is, namely Red, Blue and Yellow, from aqueous solution by adsorption. Thus, organo-bentonites containing different organic cations (para, meta or ortho) bisimidazolium dichloride (BuBIM) were prepared. The adsorption capacity of bemacide dyes with modified bentonites was carried out using two kinetic models, which are the pseudo-second order and pseudo-first order. Finally, the experimental data were compared using two isotherm equation, which are Langmuir and Freundlich.

## 2. Materials and method

### 2.1. Bentonite sample

The natural bentonite used in this study was obtained from deposits in the area of Maghnia, Algeria. The chemical composition was found to be as follows: 62.48%  $\text{SiO}_2$ , 17.53%  $\text{Al}_2\text{O}_3$ , 1.23%  $\text{Fe}_2\text{O}_3$ , 3.59%  $\text{MgO}$ , 0.82%  $\text{K}_2\text{O}$ , 0.87%  $\text{CaO}$ , 0.22%  $\text{TiO}_2$ , 0.39%  $\text{Na}_2\text{O}$ , 0.04%  $\text{As}$ , 13.0% loss on ignition at  $950^\circ\text{C}$  [16]. The mineralogical analysis showed that the native crude clay mineral contains preponderantly Montmorillonite (86 wt.%); The clay composition also

includes Quartz (10%), Cristoballite (3.0%) and Beidellite (less than 1%) [16].

The bentonite was purified and was put in sodic form according to the method published in our previous study [17]. The cation-exchange capacity (CEC) of the Na-bentonite (Na-Bt) sample was determined according to the ammonium acetate saturation method and was found to be 67.5 mg per 100 g of dry Na-Bt. The sample BET specific surface area was equal to  $52 \text{ m}^2/\text{g}$  [16].

### 2.2. Synthesis of bisimidazolium salts (BuBIM)

A mixture of bis(chloromethyl) benzene (1.748 g; 10 mmol.) and 1-butyl imidazole (2.48 g; 20 mmol.) in DMF (40 mL) were heated and stirred at  $120^\circ\text{C}$  for 8 h. A precipitate of salt was formed while the mixture was hot. After cooling ( $20^\circ\text{C}$ ), the solution was filtered under vacuum, and the solid was washed with dry diethyl ether (100 mL). The product precipitate was dried under vacuum at  $20^\circ\text{C}$  for 1 h [18].

Three salts were synthesized and characterized: para, meta and ortho ((1,4-phenylenebis(methylene))bis(1-butyl-1H-imidazol-3-ium) dichloride).

### 2.3. Preparation of organo-clays

The intercalation of the bisimidazolium cations into the bentonite galleries was carried out by cationic exchange reaction following a previously described procedure [19]: 10 g of Na-Bt are ground through 200 mesh then disperses in deionized water (200 mL). The bisimidazolium salt (0.85 g; 2.5 mmol.) will be slowly added to the bentonite suspension.

The reaction mixtures are stirred at room temperature ( $20 \pm 2^\circ\text{C}$ ) strongly for several hours (20 h). Then all products are washed free of chloride anions, separated from water; the resulting organoclays are then centrifuged at 3000 rpm for 10 min, dried in a convection oven at  $80^\circ\text{C}$  during 24 h and finally ground in an agate mortar to pass through a 200 mesh sieve.

### 2.4. Adsorption and procedure

Dye waste-waters were simulated by aqueous solutions of bemacide-series organic dyes industrially used for polyamide fibbers, namely: yellow, Red and Blue. Dyes solutions at 1000 ppm were prepared by dissolving of dyes powder (0.1 g) in 100 mL of distilled water.

The method of adsorption used for this study, was carried out by a mixture of 10 mL of dyes solutions of known

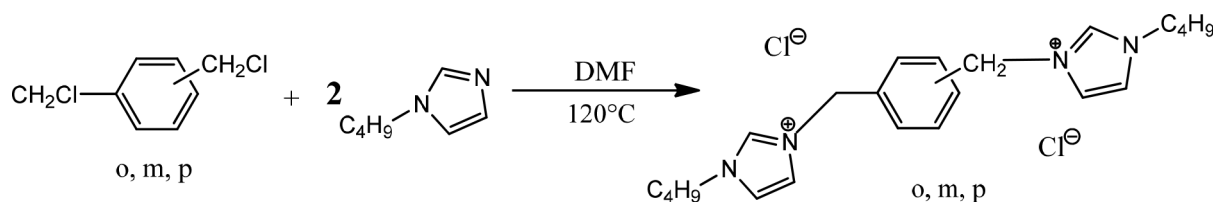


Fig. 1. Synthesis of bisimidazolium dichloride (BuBIM) (o: ortho, m: meta, p: para).

Table 1  
Characterization of bisimidazolium salts

	p.BuBIM	m.BuBIM	o.BuBIM
Yield (%)	78 %	75 %	73 %
<sup>1</sup> H NMR (D <sub>2</sub> O) δH (ppm)	0.90(CH <sub>3</sub> , 6H, m), 1.28(CH <sub>2</sub> , 4H, m), 1.84(CH <sub>2</sub> , 4H, m), 4.20(CH <sub>2</sub> , 4H, m), 5.40(CH <sub>2</sub> , 4H, d), 7.46(4H, m), 7.75(2H, d), 8.83(2H, m), 9.20(2H, s)	0.86(CH <sub>3</sub> , 6H, m), 1.29(CH <sub>2</sub> , 4H, m), 1.80(CH <sub>2</sub> , 4H, m), 4.14(CH <sub>2</sub> , 4H, m), 5.39(CH <sub>2</sub> , 4H, m), 7.54(4H, m), 7.91(2H, d), 8.82(2H, m), 9.22(2H, s)	0.93(CH <sub>3</sub> , 6H, m), 1.25(CH <sub>2</sub> , 4H, m), 1.82(CH <sub>2</sub> , 4H, m), 4.19(CH <sub>2</sub> , 4H, m), 5.51(CH <sub>2</sub> , 4H, m), 7.35(4H, m), 7.61(2H, d), 8.70(2H, m), 9.11(2H, s)
<sup>13</sup> C NMR (D <sub>2</sub> O) δC (ppm)	2C(12.56), 2C(18.70), 2C(31.14), 2C(49.46), 2C(52.32), 4C <sub>imd</sub> (122), 4C <sub>ar</sub> (129.23), 2C <sub>ar</sub> (134.70), 2C <sub>imd</sub> (135.39)	2C(12.56), 2C(18.88), 2C(31.13), 2C(49.43), 2C(52.38), 4C <sub>imd</sub> (122.33), 2C <sub>ar</sub> (128.22), 2C <sub>ar</sub> (129.17), 2C <sub>ar</sub> (130.27), 2C <sub>imd</sub> (134.78)	2C(12.57), 2C(18.75), 2C(31.24), 2C(49.57), 2C(49.98), 4C <sub>imd</sub> (122), 4C <sub>ar</sub> (131.12), 4C(135.38)
C <sub>22</sub> H <sub>32</sub> N <sub>4</sub> Cl <sub>2</sub>	Calcd. %(C 62.4, H 7.6, N 13.2) Observed %(C 62.2, H 7.8, N 13.4)	Calcd. %(C 62.4, H 7.6, N 13.2) Observed %(C 62.1, H 7.7, N 13.5)	Calcd. %(C 62.4, H 7.6, N 13.2) Observed %(C 62.3, H 7.7, N 13.3)
FTIR v (cm <sup>-1</sup> )	723–863(C–H), 1160(C–N), 1359(CH <sub>3</sub> ), 1442(C=), 1561(C–C), 1646(C=N)	733–820(C–H), 1154(C–N), 1361(CH <sub>3</sub> ), 1511(C=), 1559(C–C), 1633(C=N)	744(C–H), 1170(C–N), 1294(CH <sub>3</sub> ), 1538(C=), 1590(C–C), 1640(C=N)

concentration ( $C_0 = 50$  ppm), and 0.05 g of our bentonite in Erlenmeyer with stopper, under vigorous stirring (700 rpm) at room temperature ( $20 \pm 2^\circ\text{C}$ ). Both liquid and solid phases were separated by centrifugation; the liquid phase was controlled using UV–Vis spectrophotometer at different wave lengths: 443.5 nm for Yellow, 609.0 nm for Blue and 500.0 nm for Red.

The amount of dyes adsorbed per unit mass of adsorbent at various equilibrium times ( $q_t$ , mg/g) was calculated using following equation:

$$q_t \left( \frac{\text{mg}}{\text{g}} \right) = \frac{C_i - C_e}{W} \times V \quad (1)$$

where  $C_i$  is the initial concentration of adsorbate (mg/L),  $C_e$  is the equilibrium concentration of the adsorbate (mg/L),  $V$  is the volume of the sample (L) and  $W$  is the weight of the adsorbent (g) employed.

### 2.5. Characterization techniques

The NMR spectra were recorded in D<sub>2</sub>O, with Fourier Bruker AC 400 multi nuclear spectrometer. Elemental analyses were recorded with an automatic apparatus CHNS-O Thermo Quest. The IR spectra were obtained with solids or neat liquids with a Perkin Elmer 16 PC spectrometer Model Fourier transform infrared spectrometer.

The chemical composition of the bentonite was determined by X-ray fluorescence spectroscopy (Philips PW 3710) and XRD patterns of bentonites were collected on a Philips X-Pert diffractometer using Ni filtered Cu-K $\alpha$  radiation.

The BET-N<sub>2</sub> method was used to determine the specific surface area of bentonite, using a Volumetric Analyzer (Nova-1000). Samples containing dyes solutions were analyzed by spectrophotometer (Analytik Jena Specord 210 Plus).

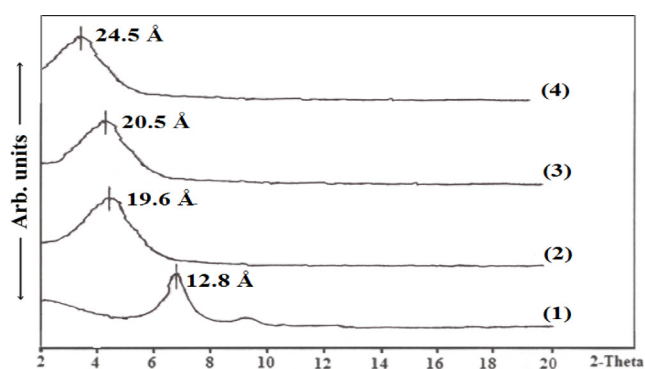


Fig. 2. XRD patterns for bentonites before and after intercalation: (001) basal peak. (1) Na-Bt; (2) o.BuBIM–Bt; (3) m.BuBIM–Bt; (4) p.BuBIM–Bt.

## 3. Results and discussion

### 3.1. XRD results of the organo-Bt

XRD is used to obtain the interlayer spacing of the bentonite, before and after modification.

The bentonite which has not been organically modified has a relatively small inter gallery distance of the  $d_{001}$  plane and the inter gallery environment is hydrophilic. Intercalation of organic surfactant between layers of bentonite not only changes the surface properties from hydrophilic to hydrophobic, but also greatly increases the basal spacing of the layers.

The X-ray diffraction pattern of Na-Bt was compared to that of the organo-Bt, as illustrated by (Fig. 2). It clearly appears that the clay mineral crystallinity of organo-Bt was not diminished upon intercalation. The Fig. 2 shows XRD pattern of crude Na-Bt, p.BuBIM–Bt, m.BuBIM–Bt and o.BuBIM–Bt were exhibiting the reflection peak occurred at  $6.9^\circ$ ,  $3.6^\circ$ ,  $4.3^\circ$  and  $4.5^\circ$ , respectively. The interlayer spacing

distance or the d-spacing of the bentonites were found to be 12.8, 24.5, 20.5 and 19.6 Å for the crude Na-Bt, p.BuBIM-Bt, m.BuBIM-Bt and o.BuBIM-Bt, respectively. The increase in the interlayer spacing of organo-Bt was due to the diffusion of organic cations into gallery regions of bentonite. The interlayer spacing obtained by using p.BuBIM molecules is more important to that obtained by using the m.BuBIM or the o.BuBIM molecules, this difference can be explained by the molecules size and their arrangement into the bentonite galleries [18].

### 3.2. Dye adsorption over Na-Bt

As a general feature, the amount of adsorbed dye increased in time. Equilibrium was attained after ca. 15 min for Bemacide-yellow, and 45 min for the two other dyestuffs (Fig. 3). The maximum adsorption capacity ( $q_{max}$ ) obtained for Bemacide-yellow (26.67) was ca. twice higher than those measured for Bemacide-red (14.7) and Bemacide-blue (13.9 mg·g<sup>-1</sup>). These values accounted for ca. 0.08 (Bemacide-yellow), 0.03 (Bemacide-red) and 0.02 mmol·g<sup>-1</sup> (Bemacide-blue), and were approximately ten times lower than the CEC value of Na-Bt. Apparently, the major part of the cation exchange sites were not involved, and dye adsorption on those located on the basal surface, if any, should be very weak. In spite of the high delamination of Na-Bt, the presence of organic dye may cause the clay mineral dispersion to coagulate, at least in part, as a result of the low dye-clay mineral affinity and of change in the distribution of the Na<sup>+</sup> ions between the Stern layer and the diffuse ionic layer [12]. This makes the basal surface to be less accessible to dye molecules. In addition, the hydrophobic character of the remaining accessible siloxane surface occurring between neighboring exchangeable cations is expected to be shaded by the presence of highly hydrophilic Na<sup>+</sup> cations [20]. This is why organic dye adsorption through aromatic rings interactions is less probable on Na-Bt.

Therefore, dye adsorption on Na-Bt must occur preponderantly via anion exchange on a small number of edge adsorption sites, as long as the latter still remains positively charged. Otherwise, only physical H-bonds or van-der-Waals interactions with the edge surface should be involved. Assuming that the dye organophilic character

increases with the number of carbon atoms; the relatively high adsorption level of Bemacide-yellow was explained in terms of better compatibility with the highly hydrophilic Na-Bt surface.

Dye adsorption was investigated in the pH range 1–7, because preliminary experiments at higher pH provided weak dye retention levels not exceeding 5 mg per gram of adsorbent. Nonetheless, because decreasing pH gave increasing amount of dye adsorbed, a special interest was focused towards the pH range 1–2 where bentonite may be prone to acid attack [12]. When necessary, prior to the experimental attempts, pH was carefully adjusted to the desired value by adding small amounts of HCl. In this pH range, very slight dealumination occurred, as supported by traces of dissolved aluminium [11,12]. Since no coagulation of Al species took place at this pH level, this process was not involved in dye removal.

From Fig. 3, pH abruptly increased within the first 1–5 min for all three dyestuffs. When contacting Na-Bt with the dye solution at its intrinsic pH, the slight excess of protons was immediately consumed in the protonation of edge OH groups and of basic oxygen atoms neighboring the exchangeable sites, inducing a quick pH increase [12,20]. In part, the buffering action of Na-Bt may also contribute, even though such a phenomenon is supposed to occur much more slowly.

#### 3.2.1. Adsorption kinetics model on Na-Bt

In an attempt to express the mechanism of dyes adsorption onto the Na-Bt, two kinetic model equations are used to analyze the adsorption experimental data for determination of the related kinetic parameters.

##### 3.2.1.1. Pseudo-first order model (PFO)

The PFO rate expression based on solid capacity is the most widely used rate equation for assigning the adsorption rate of an adsorbate from a liquid phase and is known as the Lagergren rate equation [21]. It can be written as:

$$\frac{dq}{dt} = k_f (q_e - q_t) \quad (2)$$

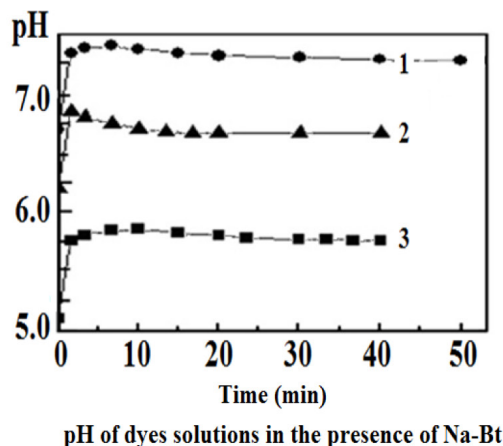
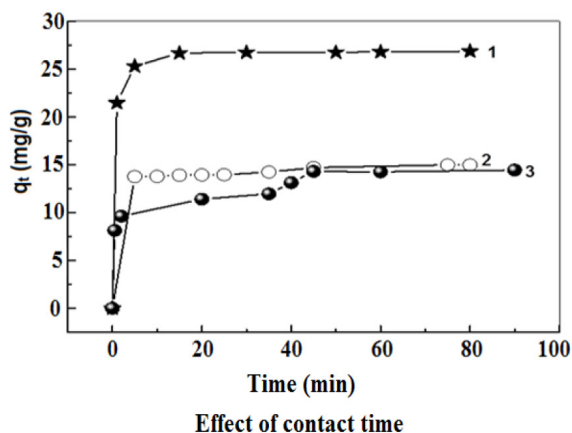


Fig. 3. Adsorption of bemacide dyes onto Na-Bt. 1: bemacide-Yellow, 2: bemacide-Red, 3: bemacide-Blue.

where  $q_t$  (mg/g) is the amount of adsorbate adsorbed at time  $t$ ,  $q_e$  (mg/g) the adsorption capacity at equilibrium,  $k_f$  ( $\text{min}^{-1}$ ) is the rate constant of the PFO model and  $t$  (min) is the time. After definite integration by applying the initial conditions:  $q_t = 0$  at  $(t = 0)$  and  $q_t = q_e$  at  $(t = t)$ , the Eq. (2) becomes:

$$\text{Log}(q_e - q_t) = \text{Log}q_e - k_f \frac{t}{2.303} \quad (3)$$

Adsorption rate constant  $K_f$  was calculated from the slope and intercept of the plots of  $\log(q_e - q_t)$  vs.  $(t)$  as displayed in Fig. 4 and the parameters are reported in Table 2.

### 3.2.1.2. Pseudo-second order model (PSO)

The pseudo-second order model can be presented in the following form [22]:

$$\frac{dq_t}{dt} = k_s (q_e - q_t)^2 \quad (4)$$

where  $k_s$  is the rate constant for the PSO model ( $\text{g/mg min}$ ). Definite integration of Eq. (4) for boundary conditions  $q_t = 0$  when  $(t = 0)$  and  $q_t = q_e$  et  $(t = t)$ , the following form of equation can be obtained:

$$\frac{t}{q_t} = \frac{1}{k_s q_e^2} + \left(\frac{t}{q_e}\right) \quad (5)$$

The initial sorption rate constant,  $h$  ( $\text{mg/g min}$ ), at  $(t = 0)$  can be defined as:  $h = k_s q_e^2$ .

Applying Eq. (5) for the analysis of kinetic data is usually based on the plotting of  $(t/q_t)$  versus  $(t)$  which should give a linear relationship; whereas,  $(1/q_e)$  and  $(1/h)$  are the slope and the intercept of obtained line, respectively.

The pseudo-first order model was more suitable to describe the adsorption kinetics of dyes onto Na-Bt. As shown in Table 2, it was observed that the high correlation coefficients are obtained when employing the pseudo-first order model ( $R^2 \geq 0.98$ ).

### 3.2.2. Adsorption isotherm modeling

The relationship between the amount of a substance adsorbed per unit mass of adsorbent at constant temperature and its concentration in the equilibrium solution is called the adsorption isotherm. The Langmuir and Freundlich isotherms are the equations most frequently used to represent the data on adsorption from solution. The Langmuir model is developed to represent chemisorption on a set of well-defined localized adsorption sites having same sorption energies independent of surface coverage and no interaction between adsorbed molecules. The Freundlich sorption isotherm gives an expression encompassing the surface heterogeneity and the exponential distribution of active sites and their energies. Langmuir and Freundlich isotherms are represented by the following equations [23,24]:

$$\frac{C_e}{q_e} = \frac{1}{q_{\max} K_L} + \frac{C_e}{q_{\max}} \quad (6)$$

$$\text{Ln}q_e = \text{Ln}K_F + \left(\frac{1}{n}\right)\text{Ln}C_e \quad (7)$$

where  $C_e$  is the equilibrium concentration of dye ( $\text{mg}\cdot\text{L}^{-1}$ ),  $q_e$  is the amount of dye adsorbed on the bentonite ( $\text{mg/g}$ ),  $K_L$  is the Langmuir adsorption constant ( $\text{L/mg}$ ),  $q_{\max}$  is the maximum amount of dye that can be adsorbed by the sodic

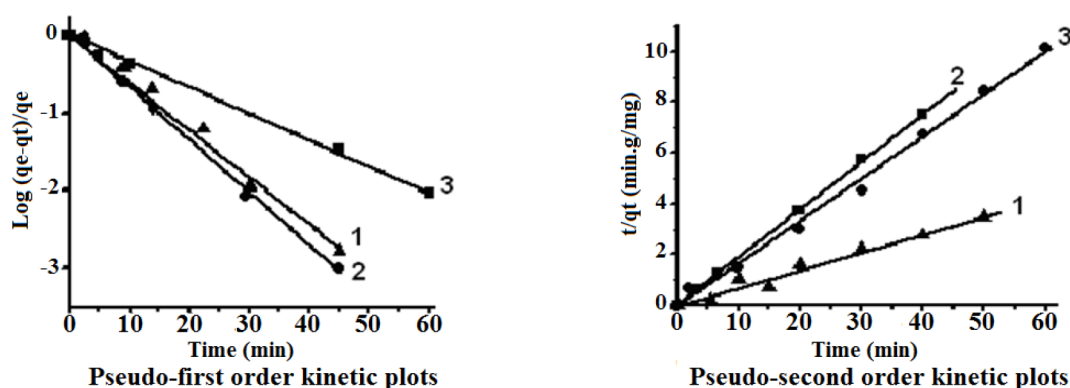


Fig. 4. Kinetic plots for the adsorption of dye onto Na-Bt. 1: bemacide-Yellow, 2: bemacide-Red, 3: bemacide-Blue.

Table 2  
Calculations of the global rate constants

Bemacide dye	Pseudo-first order		Pseudo-second order	
	$k_f$ ( $\text{min}^{-1}$ )	$R^2$	$k_s$ ( $\text{g/mg}\cdot\text{min}$ ) $10^3$	$R^2$
Yellow	0.074	0.98	0.0004	0.94
Red	0.037	0.99	0.006	0.93
Blue	0.038	0.99	0.005	0.96

bentonite,  $k_F$  is the Freundlich adsorption constant, and  $n$  is a constant that indicates the capacity and intensity of the adsorption, respectively.

The experimental data were modeled according to Langmuir and Freundlich isotherms, and the evaluated constants are given in Table 3. It was clear that Freundlich isotherm described better with a higher correlation coefficient ( $R^2 \geq 0.98$ ) in comparison with that of Langmuir ( $R^2 \leq 0.78$ ), this results confirm the existence of interactions between adsorbed molecules.

### 3.3. Adsorption on organo-Bt

#### 3.3.1. Adsorption isotherms

In the presence of organo-Bt, pH decreased during the first 10 min (Fig. 6). A possible explanation should consist in proton release upon substitution by bisimidazolium ions on the terminal  $[\text{Bt-OH}_2]^+$  groups.

The amounts of dye adsorbed increased with increasing dye concentration up to saturation (Fig. 7). All organo-Bts adsorbents showed improved capacities for dye retention. Here, the types of bisimidazolium ions and dye to be retained played key roles, inasmuch as maximum dye amounts of 168.1 (for bemacide-yellow), 154.4 (for bemacide-red) and 125.3 mg (for bemacide-blue) were adsorbed per gram of p.BuBIM-Bt, while the lowest were obtained when using m.BuBIM-Bt and o.BuBIM-Bt. Compared to Na-Bt (the maximum dye retention level did not exceed 26.7 mg/g), the use of organo-Bt for dye adsorption is more favourable. This improvement was attributed to increases in the hydrophobicity and organophilic character, increases

in interlayer spacing due to intercalation and creating of new adsorption sites. Here, hydrophobic interactions of the organic dye should be involved with both bisimidazolium cations and the remaining non-covered portion of siloxane surface [22].

The adsorption capacity obtained on p.MBIM-Bt ( $d_{001} = 24.5 \text{ \AA}$ ) is better than that obtained on m.MBIM-Bt ( $d = 20.5 \text{ \AA}$ ), the latter is better than capacity obtained on o.MBIM-Bt ( $d = 19.6 \text{ \AA}$ ). It's clear that adsorption capacity increases proportionally with interlayer distance of bentonite. The increase in the interlayer spacing of organo-Bt allows easier passage and diffusion of dye molecules in the bentonite galleries [12].

#### 3.2.2. Dye adsorption modeling

A first approach to describe the adsorption process was achieved with Langmuir's model, by plotting  $(C_e/q_e)$  (Fig. 8).

Satisfactory linearity was obtained, and the  $R^2$  values reached 0.98 for the adsorption of bemacide-yellow on o,m and p.BuBIM-Bt (Table 4). The values between 118.24 to 168.1 mg/g for the amount of an adsorbed dye monolayer ( $q_m$ ) were in agreement with the respective maximum amounts of dye adsorbed ( $Q_{max}$ ) on these organo-Bts, namely 118.24 (o.BuBIM-Bt), 141.18 (m.BuBIM-Bt) and 168.1 mg/g (p.BuBIM-Bt). Adsorption of bemacide-blue and bemacide-red did not correlate with Langmuir's model.

The Freundlich model turned out to be more adequate, inasmuch as the  $R^2$  values were highly significant, being closer to unity than those obtained in Langmuir's approach (Table 5).

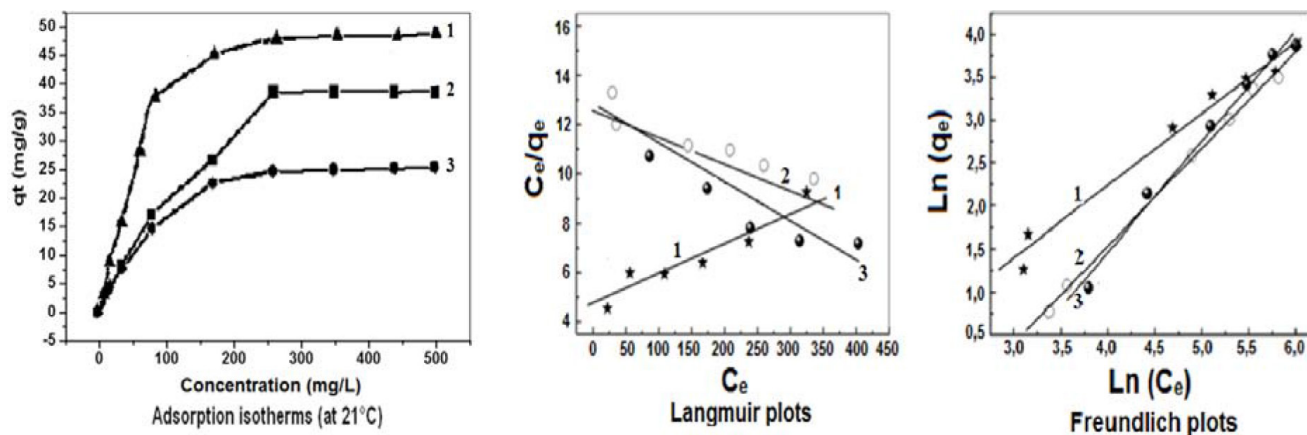


Fig. 5. Isotherms plots for the adsorption of dyes onto Na-Bt. 1: bemacide-Yellow, 2: bemacide-Red, 3: bemacide-Blue

Table 3  
Isotherm parameters for dyes adsorption onto Na-Bt

Bemacide dye	Langmuir			Freundlich		
	$q_m$ (mg/g)	$k_L$ (L/mg)	$R^2$	$n$	$k_F$ (L/mg)	$R^2$
Yellow	26.67	0.0125	0.78	1.196	0.330	0.98
Red	14.7	0.0040	0.75	0.884	0.050	0.99
Blue	13.9	0.0060	0.71	0.776	0.025	0.99

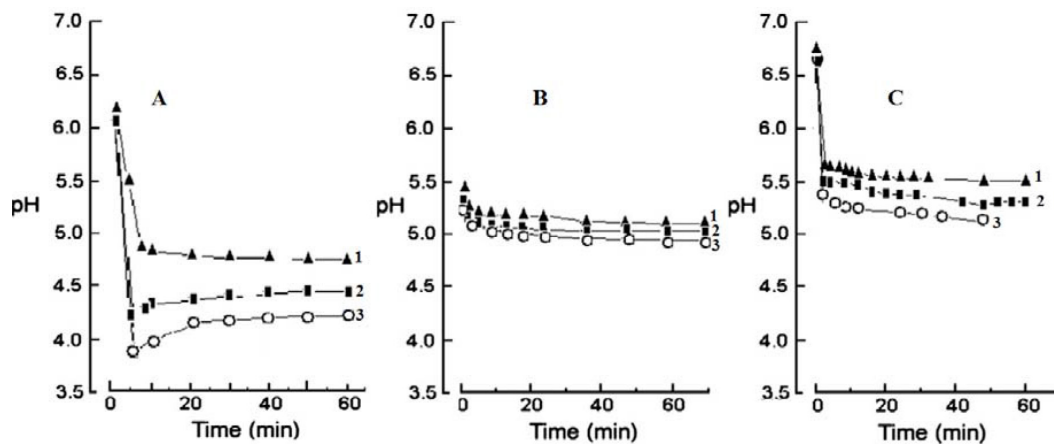


Fig. 6. pH of the dye solution in the presence of organo-Bt. 1: o.BuBIM-Bt, 2: m.BuBIM-Bt, 3: p.BuBIM-Bt. A: bemacide-yellow, B: bemacide-Red, C: bemacide-Blue.

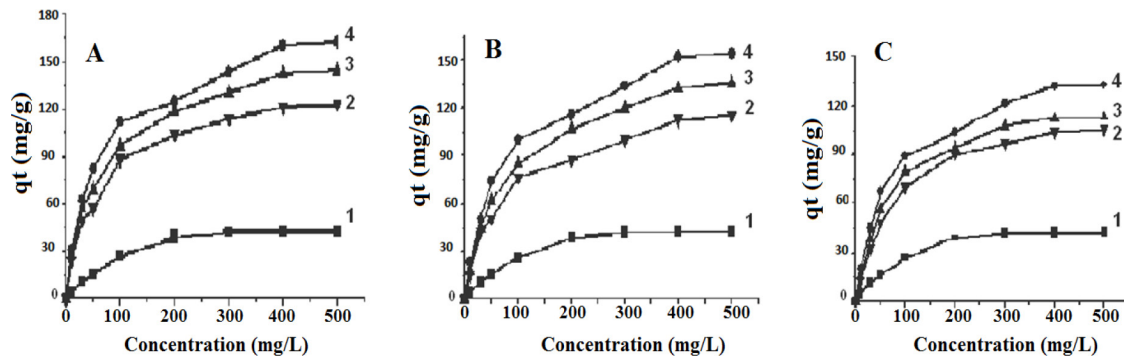


Fig. 7. Amount of adsorbed dye onto organo-Bt. A: bemacide-yellow, B: bemacide-Red, C: bemacide-Blue. 1: Na-Bt, 2: o.BuBIM-Bt, 3: m.BuBIM-Bt, 4: p.BuBIM-Bt

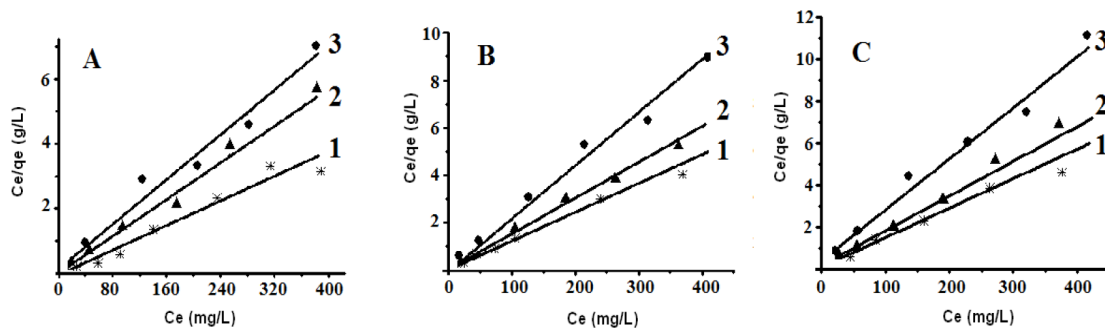


Fig. 8. Langmuir plots for the adsorption of dye onto organo-Bts. A: p.BuBIM-Bt, B: m.BuBIM-Bt, C: o.BuBIM-Bt ; 1: bemacide-Yellow, 2: bemacide-Red, 3: bemacide-Blue.

Table 4  
Langmuir parameters for dyes adsorption onto organo-Bts

Adsorbent	p.BuBIM-Bt			m.BuBIM-Bt			o.BuBIM-Bt		
	$q_m$ (mg/g)	$b$ (L/g)	$R^2$	$q_m$ (mg/g)	$b$ (L/g)	$R^2$	$q_m$ (mg/g)	$b$ (L/g)	$R^2$
Yellow	168.10	0.02	0.98	141.18	0.01	0.98	118.24	0.01	0.98
Red	154.41	0.08	0.96	126.54	0.02	0.94	108.74	0.05	0.96
Blue	125.3	0.04	0.94	105.53	0.04	0.96	98.44	0.06	0.95

Table 5  
Freundlich parameters for dyes adsorption onto organo-Bts

Adsorbent	p.BuBIM–Bt			m.BuBIM–Bt			o.BuBIM–Bt		
	<i>n</i>	<i>K</i>	<i>R</i> <sup>2</sup>	<i>n</i>	<i>K</i>	<i>R</i> <sup>2</sup>	<i>n</i>	<i>K</i>	<i>R</i> <sup>2</sup>
Yellow	0.93	1.45	0.99	0.87	1.43	0.99	0.83	1.10	0.99
Red	0.87	1.23	0.98	0.82	1.17	0.98	0.79	1.02	0.98
Blue	0.68	1.02	0.98	0.65	0.97	0.98	0.65	0.88	0.98

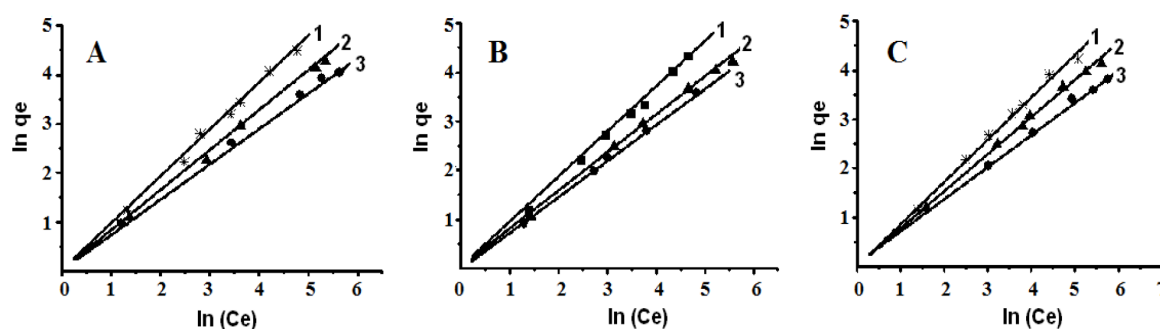


Fig. 9. Freundlich plots for the adsorption of dye onto organo-Bts. A: p.BuBIM–Bt, B: m.BuBIM–Bt, C: o.BuBIM–Bt ; 1: bemacide-Yellow, 2: bemacide-Red, 3: bemacide-Blue.

Better linearity was observed for all isotherms in the whole range of concentration investigated, when plotting  $\ln(q_e)$  as a function of  $\ln(C_e)$  (Fig. 9). This was presumably due to heterogeneity of the organo-Bts surface and to dyes–adsorbent interactions. The latter may strongly depend on the chemical structure of the dye molecules.

#### 4. Conclusion

The research was carried out in this paper clearly suggests that bisimidazolium organo-Bt acts a well adsorbent for the removal of Bemacide dyes from aqueous solutions.

Batch studies applied to bemacide dyes revealed a significant increase of the maximum adsorption capacity from 21–28 on Na-Bt to 125–168  $\text{mg}\cdot\text{g}^{-1}$  on organo-Bt. Physical adsorption may take place on Na-Bt, but stronger dye–adsorbent interactions and anion exchange on positively charged edge sites must also be involved in Bemacide-dye retention on organo-Bt. The highest adsorption capacity was noticed for bemacide-yellow dye on the p.BuMBI–Bt, presumably due higher interlayer space and better diffusion. The pseudo first-order rate equation was able to provide the best description of adsorption kinetics data for all three dyestuffs. The straight lines obtained for the Langmuir and Freundlich models obey to fit well with the experimental equilibrium data but the Freundlich model gives slightly better fitting than Langmuir model. The results show that bisimidazolium organo-bentonite could be employed as low-cost material for the removal of bemacide dyes from effluents.

#### References

- [1] K. Chinoune, K. Bentaleb, Z. Boubberka, A. Nadim, U. Maschke, Adsorption of reactive dyes from aqueous solution by dirty bentonite, *Appl. Clay Sci.*, 123 (2016) 64–75.
- [2] S.P. Patil, B. Bethi, G.H. Sonawane, V.S. Shrivastava, S. Sonawane, Efficient adsorption and photo catalytic degradation of Rhodamine B dye over  $\text{Bi}_2\text{O}_3$ -bentonite nano composites: A kinetic study, *J. Ind. Eng. Chem.*, 34 (2016) 356–363.
- [3] A. Ozcan, O. Cigdem, E. Yunus, A.S. Ozcan, Modification of bentonite with a cationic surfactant: An adsorption study of textile dye Reactive Blue 19, *J. Hazard. Mater.*, 140 (2007) 173–179.
- [4] L. Zhang, P. Hu, J. Wang, R. Huang, Adsorption of Amido Black 10B from aqueous solutions onto Zr (IV) surface-immobilized cross-linked chitosan/bentonite composite, *Appl. Surf. Sci.*, 369 (2016) 558–566.
- [5] P.K. Malik, Use of activated carbons prepared from sawdust and rice-husk for adsorption of acid dyes: a case study of Acid Yellow 36, *Dyes Pigm.*, 56 (2003) 239–249.
- [6] H. Li, Y. Leng, X. Tuo, Research on adsorption and desorption Behavior of Pu on bentonites for buffer backfill material, *Procedia Environ. Sci.*, 31 (2016) 401–407.
- [7] L. Zhang, P. Hu, J. Wang, Q. Liu, R. Huang, Adsorption of methyl orange (MO) by Zr (IV)-immobilized cross-linked chitosan/bentonite composite, *Int. J. Biol. Macromolec.*, 81 (2015) 818–827.
- [8] D. Wan, W. Li, G. Wang, K. Chen, L. Lu, Q. Hu, Adsorption and heterogeneous degradation of rhodamine B on the surface of magnetic bentonite material, *Appl. Surf. Sci.*, 349 (2015) 988–996.
- [9] B. Li, L.Y. Li, J.R. Grace, Adsorption and hydraulic conductivity of landfill-leachate perfluorinated compounds in bentonite barrier mixture, *J. Environ. Manag.*, 156 (2015) 236–243.
- [10] B. Makhoukhi, M.A. Didi, D. Villemin, A. Azzouz, Acid activation of Bentonite for use as a vegetable oil bleaching agent, *Int. J. Fats Oils*, 60 (2009) 343–349.
- [11] B. Makhoukhi, M.A. Didi, H. Moulessehou, A. Azzouz, Telen dye removal from Cu(II)-containing aqueous media using p-diphosphonium organo-montmorillonite, *Med. J. Chem.*, 2 (2011) 44–55.
- [12] B. Makhoukhi, M.A. Didi, H. Moulessehou, A. Azzouz, D. Villemin, Diphosphonium ion-exchanged montmorillonite for Telen dye removal from aqueous media, *Appl. Clay Sci.*, 50 (2010) 354–361.

- [13] V.K. Gupta, M. Sharma, R.K. Vyas, Hydrothermal modification and characterization of bentonite for reactive adsorption of methylene blue: An ESI-MS study, *J. Environ. Chem. Eng.*, 3 (2015) 2172–2179.
- [14] S.W. Karichoff, S. Browns, Sorption of hydrophobic pollutants on natural sediment, *Water Res.*, 13 (1979) 241–250.
- [15] R. Huang, B. Wang, B. Yang, D. Zheng, Z. Zhang, Equilibrium, kinetic and thermodynamic studies of adsorption of Cd(II) from aqueous solution onto HACC–bentonite, *Desal. Wat. Treat.*, 280 (2011) 297–304.
- [16] M.A. Didi, B. Makhoukhi, A. Azzouz, D. Villemain, Colza oil bleaching through optimized acid activation of bentonite-A comparative study, *Appl. Clay Sci.*, 42 (2009) 336–344.
- [17] B. Makhoukhi, D. Villemain, M.A. Didi, Synthesis of bisimidazolium–ionic liquids: Characterization, thermal stability and application to bentonite intercalation, *J. Taibah Univ. Sci.*, 10 (2016) 168–180.
- [18] B. Makhoukhi, M.A. Didi, D. Villemain, Preparation, characterization and thermal stability of bentonite modified with bisimidazolium salts, *Mater. Chem. Phys.*, 138 (2013) 199–203.
- [19] B. Makhoukhi, M.A. Didi, D. Villemain, Modification of bentonite with diphosphonium salts: Synthesis and characterization, *Mater. Lett.*, 62 (2008) 2493–2496.
- [20] A. Mehmet, The removal of phenolic compounds from aqueous solutions by organophilic bentonite, *J. Colloid Interface Sci.*, 280 (2004) 299–304.
- [21] J. Su, S. Lin, Z. Chen, M. Megharaj, R. Naidu, Dechlorination of p-chlorophenol from aqueous solution using bentonite supported Fe/Pd nano particles: Synthesis, characterization and kinetics, *Desal. Wat. Treat.*, 280 (2011) 167–173.
- [22] B. Makhoukhi, M. Djab, M.A. Didi, Adsorption of Telon dyes onto bis-imidazolium modified bentonite in aqueous solutions, *J. Env. Chem. Eng.*, 3 (2015) 1384–1392.
- [23] I. Langmuir, The evaporation, condensation and reflection of molecules and the mechanism of adsorption, *J. Franklin Inst.*, 217 (1934) 543–569.
- [24] H. Freundlich, Concerning adsorption in solutions, *Zeitschrift Fur Phys. Chemie-Stoichiomet. Verwandt.*, 57 (1906) 385–470.